AIAA JOURNAL
Vol. 33, No. 12, December 1995

Toward the Direct Calculation of Noise: Fluid/Acoustic Coupled Simulation

K. Viswanathan*
Lockheed Martin Aeronautical Systems, Marietta, Georgia 30064-0685
and
L. N. Sankar†
Georgia Institute of Technology, Atlanta, Georgia 30332

A numerical technique for the direct calculation of flow generated noise is developed in this paper and applied to the prediction of supersonic jet noise. In this approach, each flow parameter is decomposed into a time-averaged mean and a time-dependent fluctuating part. The mean flow is established with the solution of the three-dimensional compressible Navier–Stokes equations in the first step. Flow perturbations based on the description of the large-scale structures as a linear superposition of normal mode instability waves are introduced at the nozzle exit plane. Their propagation in time and space are studied through solution of the Euler equations for the perturbations in the second step. Such an approach ensures that the fluctuation variables, which may be several orders of magnitude smaller than the mean values, are computed accurately without numerical round-off errors. Some dynamic features of the jet flow are presented. Predictions of radiated noise for a few test cases and qualitative comparisons with experiments are made. Effects of jet temperature on the peak directivity of the radiated sound are examined.

Nomenclature

$\boldsymbol{A}, \boldsymbol{B}$	= Jacobian matrices in curvilinear coordinate system
$\tilde{\boldsymbol{A}}, \tilde{\boldsymbol{B}}, \tilde{\boldsymbol{C}}$	= Jacobian matrices in Cartesian coordinate system
$A(x)$	= amplitude of instability wave
b	= half-velocity thickness of mixing layer
$\boldsymbol{E}, \boldsymbol{F}, \boldsymbol{G}$	= inviscid flux vectors in curvilinear coordinate system
$\boldsymbol{E}_v, \boldsymbol{F}_v, \boldsymbol{G}_v$	= viscous flux vectors in curvilinear coordinate system
$\tilde{\boldsymbol{E}}, \tilde{\boldsymbol{F}}, \tilde{\boldsymbol{G}}$	= inviscid flux vectors in Cartesian coordinate system
$\boldsymbol{I}$	= identity matrix
i	= imaginary number, $\sqrt{(-1)}$
M_j	= jet Mach number
m	= azimuthal mode number
p	= pressure
$\boldsymbol{Q}$	= flow properties vector in curvilinear coordinate system
$\tilde{\boldsymbol{Q}}$	= nonlinear fluctuation terms
$\boldsymbol{q}$	= flow properties vector in Cartesian coordinate system
$\tilde{\boldsymbol{R}}, \tilde{\boldsymbol{S}}, \tilde{\boldsymbol{T}}$	= viscous flux vectors in Cartesian coordinate system
(r, θ, x)	= cylindrical polar coordinate system
r_j	= radius of jet
t, τ	= time
u, v, w	= velocities in polar coordinate system
(x, y, z)	= Cartesian coordinate system
α	= eigenvalue
δ	= difference operator
(ξ, η, ζ)	= curvilinear coordinate system
ρ	= density
ϕ	= any flow variable
ω	= radian frequency

Subscripts

i, j, k	= grid indices
j	= jet
x, y, z, t	= derivatives in Cartesian coordinate system
ξ, η, ζ, τ	= derivatives in curvilinear coordinate system

Superscripts

$n, (n+1)$	= time levels
$\bar{}$	= time-averaged quantity
$'$	= fluctuation quantity
$\hat{}$	= eigenfunction

Introduction

RECENT efforts to develop a supersonic civil transport plane and the proposed stringent community noise requirements have led to a resurgence of interest in the prediction and suppression of noise radiated by supersonic jets. Considerable attention has been focused on developing reliable prediction methods, especially for the dominant supersonic jet component. Direct numerical solution of the Navier–Stokes equations would provide the radiated noise, but this approach is not practical because of the limitations of the present day computers. Three different approaches have been adopted for the predictions of jet noise in the past: empirical schemes, theoretical/analytical methods, and numerical simulation through Navier–Stokes equations. In the empirical approach, the far-field noise is directly correlated to the mean flow parameters using Lighthill's acoustic analogy or through the use of empirical relations. Classical theoretical methods involve the modeling or calculation of the source term from simplified equations and the application of the acoustical analogy for noise predictions. Recent theoretical/analytical methods are based on the observations of Tam and Morris[1] and Tam and Burton,[2] among others, that the noise producing structures in supersonic shear layers may be modeled as instability waves. Based on the instability wave theory, these researchers were able to predict the noise characteristics of high-speed circular and noncircular jets. Recently, Tam[3] and Tam and Chen[4] have developed stochastic model theories for broadband shock associated noise and turbulent mixing noise from high-speed jets. Very good agreement with experimental measurements were obtained with these theories.

Received Dec. 8, 1994; revision received June 21, 1995; accepted for publication June 29, 1995.

*Senior Engineer, Propulsion and Acoustics Department. Member AIAA.
†Professor, School of Aerospace Engineering.

In the computational fluid dynamics (CFD) and computational aeroacoustics arenas, several recent studies have focused on the direct calculation of radiated noise from the governing equations, without taking recourse to Lighthill's acoustic analogy, e.g., Scott.[5] In most of these studies, the mean flowfield is established with the solution of the Navier–Stokes equations. The radiated noise is obtained by extending the solution to the far field throughlinearized Euler equations[6] or with the acoustic analogy.[7] The many pitfalls associated with extending CFD techniques to acoustic analysis are well documented. Numerical schemes that possess minimum dissipation, minimum dispersion, and isotropy are necessary for acoustic applications and are currently being developed. Because of the prohibitive cost of direct calculation of noise from the Navier–Stokes equations, and the conflicting requirements for the accurate calculation of both the viscous flow and the acoustic field, it is preferable to carry out a two-part calculation. Such an approach has been adopted by Bechara et al.[8] in their development of a stochastic noise generation and radiation model. In the first step, the mean flowfield and the turbulent components are evaluated while the acoustic perturbations are neglected. In the second step, a set of governing equations for the acoustic variables is solved. This procedure was applied to a subsonic freejet, and the incompressible Euler equations were solved, with the turbulence field represented by a synthesis of a collection of discrete Fourier modes. Good comparisons with experiments were reported.

In the present study, a numerical technique that utilizes the calculated mean flowfield for the prediction of radiated noise is described. The mean flowfield is first obtained from the solution of the Navier–Stokes equations in the jet and in the immediate vicinity. The solution is extended to the near field through the Euler equations for flow fluctuations. This approach may be viewed as a cross between a classical linear stability analysis and CFD techniques. As in a stability analysis, the flow variables are decomposed into two parts, and a system of equations for the fluctuations are obtained for a given mean flow. On the left-hand side of this system of equations are the linearized Euler equations. The right-hand side contains source terms that are related to the turbulent fluctuations and their interactions with the mean flow. After the equations are derived, the spatial derivatives in this equation set are discretized on a curvilinear grid using CFD-based techniques. The resulting system of ordinary differential equations for the flow perturbations is solved by direct numerical integration in time. Information such as temporal and spatial growth of disturbances introduced into the shear layer, convective speeds of instability waves, and the directivity of the radiated noise, are all extracted directly from the time–space domain solution, using data processing techniques similar to that employed by experimenters.

There are several drawbacks when the desirable features of the stability theory are combined with computational fluid dynamics techniques. The numerical viscosity in modern finite difference schemes and temporal damping associated with any stable time-marching scheme could reduce the accuracy of the solution, particularly when coarse grids and/or large time step values are employed. A minimum of 10 points per wave length are usually needed to faithfully capture acoustic waves propagating in space. As a result, such solutions are at least two orders of magnitude more expensive than existing analytical techniques. But the mean flow may be unsteady, nonuniform, nonparallel, and may contain embedded shocks and embedded solid surfaces. The present approach is suitable for these kinds of flows. Furthermore, the prescription of the mean flowfield in terms of simple analytic functions for noncircular geometries poses a problem, in the evaluation of noise using stability theory. In a recent study, Dahl and Morris[9] used the mean flowfield obtained from the solution of the compressible Reynolds-averaged boundary-layer equations together with the instability wave formulation of Tam and Burton[2] for the evaluation of noise from coaxial jets. The mean flow computed from parabolized Navier–Stokes (PNS) solvers[10] or a large eddy simulation (LES) solver[7] could serve as the input for noise calculations using Euler equations. This approach permits the analysis of a variety of flows, such as flow through ejectors, elliptic and rectangular geometries, etc. The near-field solutions from the Euler equations may then be used in a Kirchhoff formulation for the estimation of far-field noise.[11,12]

This work is organized as follows. First, the Navier–Stokes solver used to solve the Reynolds-averaged mean flow equations is described. The three-dimensional Euler equations for flow perturbations are derived on a Cartesian coordinate system, and techniques are described and developed for the discretization of these equations on a general curvilinear coordinate system. Some code validation studies for the jet mean flowfield are presented. Finally, the current approach is applied to the prediction of mixing noise generated by an axisymmetric, perfectly expanded, supersonic jet. It should be noted that the main goal of this study is to demonstrate the validity and usefulness of the current approach, rather than make direct comparisons with experiments. The noise calculations are restricted to axisymmetric disturbances in light of computer needs. The attendant limitations are discussed. Nevertheless, the directional features of the radiated noise are expected to be resolved by the simpler computations. This paper reports our efforts to couple the aerodynamic and aeroacoustic solutions and represents one of the first attempts in the development of a numerical technique for the direct calculation of radiated noise.

Mathematical Formulation

Navier–Stokes Formulation

The vector form of the full Reynolds-averaged, three-dimensional Navier–Stokes equations based on an arbitrary curvilinear coordinate system may be written as

$$\boldsymbol{Q}_\tau + (\boldsymbol{E} - \boldsymbol{E}_v)_\xi + (\boldsymbol{F} - \boldsymbol{F}_v)_\eta + (\boldsymbol{G} - \boldsymbol{G}_v)_\zeta = 0 \tag{1}$$

where $\boldsymbol{Q}$ is the vector of unknown flow properties.

The time derivative $\boldsymbol{Q}_\tau$ of Eq. (1) is approximated using two-point backward difference at the new time level,

$$\boldsymbol{Q}_\tau = (\boldsymbol{Q}^{n+1} - \boldsymbol{Q}^n)/\Delta\tau \tag{2}$$

where n refers to the time level at which all quantities are known and $n+1$ is the new time level. All spatial derivatives are approximated by standard fourth-order central differences and are represented by the differencing operators δ, e.g., $\boldsymbol{E}_\xi \simeq \delta_\xi \boldsymbol{E}$.

The derivative in the azimuthal direction $\boldsymbol{F}_\eta$ is evaluated explicitly at the old time level n, but we use the values at time level $n+1$ as soon as they become available. This semiexplicit treatment of the η derivative enables one to solve implicitly for all points at one azimuthal plane at a time.

The viscous terms $\boldsymbol{E}_v$, $\boldsymbol{F}_v$, and $\boldsymbol{G}_v$ are evaluated explicitly, using half-point central differencing, so that the computational stencil for the stress terms uses only three nodes in each of the three directions. Explicit treatment of the stress terms still permits the use of large time steps since the Reynolds numbers of interest here are fairly large.

The time and space discretizations just described lead to a system of nonlinear, block pentadiagonal matrix equations for the unknown $\boldsymbol{Q}^{n+1}$. The equation is then linearized using the Jacobian matrices $\boldsymbol{A} = \partial\boldsymbol{E}/\partial\boldsymbol{Q}$ and $\boldsymbol{B} = \partial\boldsymbol{G}/\partial\boldsymbol{Q}$ and approximately factored into a product of two block tridiagonal matrix equations,

$$[\boldsymbol{I} + \Delta\tau\delta_\xi \boldsymbol{A}][\boldsymbol{I} + \Delta\tau\delta_\eta \boldsymbol{B}]\Delta\boldsymbol{Q} = \boldsymbol{R}$$

$$= -\Delta\tau[\delta_\xi(\boldsymbol{E} - \boldsymbol{E}_v) + \delta_\eta(\boldsymbol{F} - \boldsymbol{F}_v) + \delta_\zeta(\boldsymbol{G} - \boldsymbol{G}_v)] \tag{3}$$

The use of standard central differences to approximate the spatial derivatives could give rise to the growth of high-frequency errors with time. To control this growth, a set of second/fourth-order nonlinear, spectral radius-based, explicit artificial dissipation terms are added to the discretized equations. A second-order implicit dissipation is used to help the overall numerical stability of the scheme.

Two different turbulence models, an algebraic eddy viscosity model and a k–ε model, have been implemented in the mean flow solver. The algebraic eddy viscosity model that models the eddy viscosity as being proportional to the shear layer thickness d and the velocity difference across the shear layer ΔU is used. The jet flowfield is divided into three regions: initial mixing region where mixing is confined to the shear layer, a transition region, and a fully developed regime. The empirical constants that appear in the

algebraic eddy viscosity model were adjusted in the three regimes to give good predictions for the centerline velocity and temperature variation for subsonic and supersonic heated jets. Once a set of suitable constants were found, these empirical constants were frozen for all subsequent studies.

Aeroacoustic Formulation

The computational aeroacoustic formulation starts with the three-dimensional compressible Navier–Stokes equations in a Cartesian coordinate system,

$$q_t + \tilde{E}_x + \tilde{F}_y + \tilde{G}_z = \tilde{R}_x + \tilde{S}_y + \tilde{T}_z \tag{4}$$

where $\tilde{E}, \tilde{F}$, and $\tilde{G}$ contain information about the mass, momentum, and energy fluxes, pressure forces, and work done by pressure forces; $\tilde{R}, \tilde{S}$, and $\tilde{T}$ represent viscous stress and heat diffusion contributions. The flow variables are decomposed into a mean flow component and a perturbation component,

$$q = \bar{q} + q' \tag{5}$$

The Cartesian flux terms E, F, G, etc., may be expressed in terms of the mean flow and the perturbation quantities, while retaining complete nonlinearity. For example, one may write

$$\rho u = \bar{\rho}\bar{u} + \bar{\rho}u' + \bar{u}\rho' + \rho' u' \tag{6}$$

These decompositions are substituted into Eq. (4), and the unsteady Euler equations for the mean flow are subtracted. If the contributions of q' to the viscous terms on the right-hand side of Eq. (4) are neglected, the following form results:

$$(q')_t + (\tilde{A}q')_x + (\tilde{B}q')_y + (\tilde{C}q')_z = \tilde{Q} \tag{7}$$

The matrices $\tilde{A}, \tilde{B}$, and $\tilde{C}$ are the Jacobians of the fluxes $\tilde{E}, \tilde{F}$, and $\tilde{G}$, respectively, and are computed using the mean flow information,

$$\tilde{A} = \frac{\partial \tilde{E}}{\partial q}, \qquad \tilde{B} = \frac{\partial \tilde{F}}{\partial q}, \qquad \tilde{C} = \frac{\partial \tilde{G}}{\partial q} \tag{8}$$

The quantity $\tilde{Q}$ contains the nonlinear terms. If these terms are neglected, a linear formulation results. The present procedure has been implemented in the computer code such that either the linear form or the full nonlinear form may be solved. The mean flow quantities may be several orders of magnitude larger than the perturbation quantities, especially outside the jet. The separation of the flowfield into two components will ensure that the mean flow will not overwhelm q' and lead to numerical round-off.

Finite Volume Discretization

Consider a control volume surrounding the node (i, j, k) as shown in Fig. 1. Equation (7) may be cast in an integral form on such a control volume, and the application of the divergence theorem yields the following relation:

$$\int_V \frac{\partial q'}{\partial t}\,dV + \oint\!\!\oint_S [\tilde{A}q'\hat{i} + \tilde{B}q'\hat{j} + \tilde{C}q'\hat{k}] \cdot \hat{n}\,dS = \int_V \tilde{Q}\,dV \tag{9}$$

The surface integral is performed over the six faces of the control volume here. Assuming that the coefficient matrices $\tilde{A}, \tilde{B}$, and $\tilde{C}$ (which are only functions of the mean flow $\bar{q}$) could be computed at the centers of the cell faces, the preceding equation may be written

$$\mathrm{Vol}_{i,j,k}\left[\frac{dq'}{dt}\right]_{i,j,k} + \sum \{[\tilde{A}\hat{i} + \tilde{B}\hat{j} + \tilde{C}\hat{k}] \cdot n\Delta S\} q' = \mathrm{Vol}_{i,j,k}[\tilde{Q}]_{i,j,k} \tag{10}$$

where $\mathrm{Vol}_{i,j,k}$ is the volume of the control volume, $\hat{n}$ the outward facing unit normal at each of the six faces, and ΔS the area of the cell faces. Equation (10) may be written in the following convenient form:

$$\mathrm{Vol}_{i,j,k}\left[\frac{dq'}{dt}\right]_{i,j,k} + \sum Pq' = \mathrm{Vol}_{i,j,k}[\tilde{Q}]_{i,j,k} \tag{11}$$

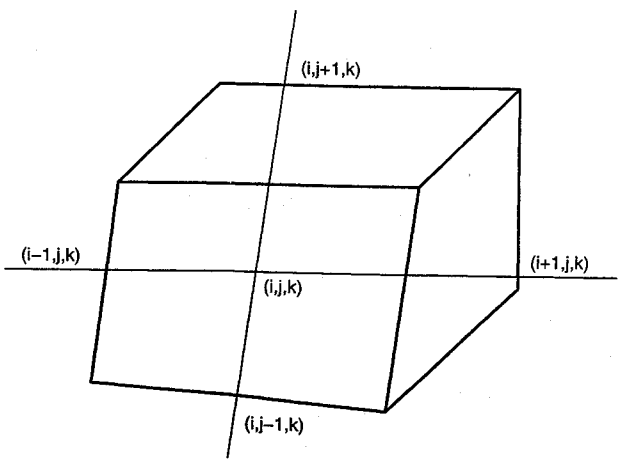

Fig. 1 Sketch of control volume.

Solution Procedure

Numerical Scheme

The numerical algorithm used to advance the flow properties in time is described in this section. Satisfactory numerical approximations to the flux vector Pq' crossing each of the six faces may be computed in several ways. This leads to a number of numerical schemes, such as upwind schemes, the classical MacCormack scheme, and central (symmetric) difference schemes. Sankar et al.[13] have compared the relative merits of these schemes for a number of classical two-dimensional acoustics problems. The central difference schemes require the addition of artificial viscosity in order to obtain stable solutions. The jet noise simulation solver has several options implemented, a third-order upwind scheme, and a second/fourth-order MacCormack scheme. The upwind schemes were found to be too dissipative and, hence, deemed unsuitable for the current application. For the results presented in this paper, the explicit two–four MacCormack scheme of Gottlieb and Turkel[14] has been employed. During the predictor step, the following form of the discretized equation is solved:

$$\begin{aligned} q'|^p_{i,j,k} = q'|^n_{i,j,k} &- \Delta t\left[\frac{7\tilde{F}'_{i,j,k} - 8\tilde{F}'_{i-1,j,k} + \tilde{F}'_{i-2,j,k}}{6\Delta x}\right]^n \\ &- \Delta t\left[\frac{7\tilde{G}'_{i,j,k} - 8\tilde{G}'_{i,j-1,k} + \tilde{G}'_{i,j-2,k}}{6\Delta y}\right]^n \\ &- \Delta t\left[\frac{7\tilde{H}'_{i,j,k} - 8\tilde{H}'_{i,j,k-1} + \tilde{H}'_{i,j,k-2}}{6\Delta z}\right]^n + \Delta t\tilde{Q}^n_{i,j,k} \end{aligned} \tag{12}$$

where $\tilde{F}' = \tilde{A}q', \tilde{G}' = \tilde{B}q', \tilde{H}' = \tilde{C}q'$.

During the corrector step, the following form is used:

$$\begin{aligned} q'|^{n+1}_{i,j,k} = &\frac{q'|^n_{i,j,k} + q'|^p_{i,j,k}}{2} \\ &+ \Delta t\left[\frac{7\tilde{F}'_{i,j,k} - 8\tilde{F}'_{i+1,j,k} + \tilde{F}'_{i+2,j,k}}{12\Delta x}\right]^p \\ &+ \Delta t\left[\frac{7\tilde{G}'_{i,j,k} - 8\tilde{G}'_{i,j+1,k} + \tilde{G}'_{i,j+2,k}}{12\Delta y}\right]^p \\ &+ \Delta t\left[\frac{7\tilde{H}'_{i,j,k} - 8\tilde{H}'_{i,j,k+1} + \tilde{H}'_{i,j,k+2}}{12\Delta z}\right]^p + \frac{\Delta t}{2}\left[\tilde{Q}^p_{i,j,k}\right] \end{aligned} \tag{13}$$

The spatial derivatives in the nonlinear term $\tilde{Q}$ are also computed using appropriate one-sided differences during the predictor and the corrector stages.

Unlike the upwind schemes, the MacCormack scheme does not have a sufficient amount of built-in dissipation to eliminate high-frequency spatial oscillations. An explicit fourth-order filter is, therefore, added to the right-hand side of Eq. (13) during both the predictor and corrector steps to eliminate such nonphysical oscillations. This filter is of the form

$$\begin{aligned} &-\psi[q'_{i+2} - 4q'_{i+1} + 6q'_i - 4q'_{i-1} + q'_{i-2}] \\ &-\psi[q'_{j+2} - 4q'_{j+1} + 6q'_j - 4q'_{j-1} + q'_{j-2}] \\ &-\psi[q'_{k+2} - 4q'_{k+1} + 6q'_k - 4q'_{k-1} + q'_{k-2}] \end{aligned} \tag{14}$$

where ψ is a coefficient of the order of (1/64).

Inflow Conditions

There is substantial experimental and theoretical evidence that the dominant part of the turbulent mixing noise from supersonic jets is generated by the large-scale turbulent structures of the jet flow. Tam[15] has provided a detailed review of the noise generated by the coherent structures. When these structures are convected at supersonic speeds with respect to the ambient speed of sound, they serve as efficient noise generators. The experimental studies of McLaughlin et al.,[16] Morrison and McLaughlin,[17] and Troutt and McLaughlin[18] in low and moderate Reynolds number supersonic jets indicated that the large-scale structures took the form of instability waves of discrete frequencies at low Reynolds number and consisted of a band of instability waves at higher Reynolds numbers. Comparisons of these data with high Reynolds number experiments (see Seiner et al.[19]) suggested that the characteristics of the large-scale structures in high Reynolds number supersonic jets are probably similar to those of the instability waves at lower Reynolds numbers. Tam et al.[20] demonstrated that the highest sound pressure levels of the far-field noise occurs at a direction and frequency that closely match the Mach wave direction and frequency of the most amplified instability wave of the jet. This study is mainly concerned with the Mach wave emission process and, therefore, the flow properties associated with the large-scale structures are specified as inflow conditions. The large-scale structures are modeled as a superposition of the normal mode instability waves, consisting of the fundamental frequency, which is the most amplified frequency close to the nozzle exit, and its subharmonics. Such a description, based on the experimental observations of Ho and Huang,[21] has been to shown to capture the dynamic evolution of free shear layers, see Morris et al.[22] and Viswanathan and Morris.[23] The form of the wavelike fluctuations is taken to be

$$\phi'(r, \theta, x, t) = \Re\{A(x)\hat{\phi}(r) \exp[i(\alpha x + m\theta - \omega t)]\} \tag{15}$$

where $\Re$ denotes the real part of a function.

Perturbations of this form are introduced into the Euler equations. Elimination of all of the flow variables in favor of the pressure fluctuation yields the Rayleigh equation,

$$\begin{aligned} &\frac{d^2\hat{p}}{dr^2} + \left[\frac{1}{r} - \frac{1}{\bar{\rho}}\frac{d\bar{\rho}}{dr} + \frac{2\alpha}{(\omega - \alpha\bar{u})}\frac{d\bar{u}}{dr}\right]\frac{d\hat{p}}{dr} \\ &+ \left[\bar{\rho}M_j^2(\omega - \alpha\bar{u})^2 - \frac{m^2}{r^2} - \alpha^2\right]\hat{p} = 0 \end{aligned} \tag{16}$$

The overbar in Eq. (16) denotes a mean quantity. The axial wave number for a given frequency is obtained through the solution of the compressible Rayleigh equation. Details of the stability analysis are given in Tam and Morris[1] and Tam and Burton.[2] The eigenfunctions for other fluctuating flow variables are easily obtained from the Euler equations. A normalization condition for the eigenfunctions is imposed such that

$$\int_0^\infty \left[\frac{1}{4}\bar{\rho}\bar{u}(|\hat{u}|^2 + |\hat{v}|^2|\hat{w}|^2) + \frac{\bar{u}M_j^2}{4\bar{\rho}}|\hat{p}|^2 + \frac{1}{2}\Re(\hat{p}\hat{u}^*)\right] \cdot r\,dr = 1 \tag{17}$$

where the asterisk denotes the complex conjugate of a function. The initial conditions are specified as the sum of the eigenfunctions for the different frequencies used to model the large-scale structures and may be written

$$\phi'(r, \theta, x, t) = \sum_{l=1}^{N} \Re\{A_l(x_0)\hat{\phi}_l(r, \omega_l, m) \exp[i(m\theta - \omega_l t)]\} \tag{18}$$

The initial-half velocity thickness of the annular mixing layer, b/r_j, is taken to be 0.05 and the eigenfunctions are prescribed at a small distance downstream of the nozzle exit. This manner of forcing the flow at the upstream boundary is expected to characterize the large-scale structures and provide the directivity features of the radiated noise.

Numerical Results and Discussion

In this section, some of the details and results of the mean flow simulations are described first. Predictions of radiated noise from the Euler equations are then presented.

Mean Flow Prediction

An accurate simulation of the mean flowfield is the first requisite in the computation of the radiated noise. The three-dimensional Navier–Stokes equations are solved on an axisymmmetric grid, consisting of three azimuthal planes. The computations are performed on the centerplane, and the two adjacent planes are used to enforce axisymmetry at each time step. A cylindrical grid which consists of 251 nodes in the axial direction, 81 nodes in the radial direction, and 3 planes in the azimuthal direction, is employed. A schematic of the computational domains for the mean flow and the acoustic calculations is illustrated in Fig. 2. A fine grid is prescribed close to the jet exit plane, and the grid spacing is gradually increased in a geometric fashion as the distance from the nozzle exit increases in both the axial and radial directions. Dash et al.[24] have evaluated the performance and suitability of different turbulence models for high-speed jet flows. No single model with universal coefficients has been found to be suitable for different types of flows. Two different turbulence models, a simple algebraic eddy viscosity model and a two-equation k–ε model, are considered. Based on the recommendations of Dash et al.,[24] a k–ε model with the centerline correction proposed by Pope[25] and compressibility correction was incorporated. Extensive measurements of the mean flowfield and the acoustic characteristics of high-temperature supersonic jets at NASA Langley by Seiner et al.[26] are chosen as the test cases and considered for detailed study. The performance of the k–ε model was assessed through comparison of the mean flow characteristics with measurements. Several problems, such as the specification of the initial turbulent kinetic energy values, maximum cap on k to prevent unstable solutions, etc., were encountered. The predicted centerline characteristics were not good due to the cited problems. The main goal of this study is the calculation of the radiated noise from a computed mean flowfield and not the development of an accurate turbulence model. In light of this objective, it was decided to employ the simpler eddy viscosity model.

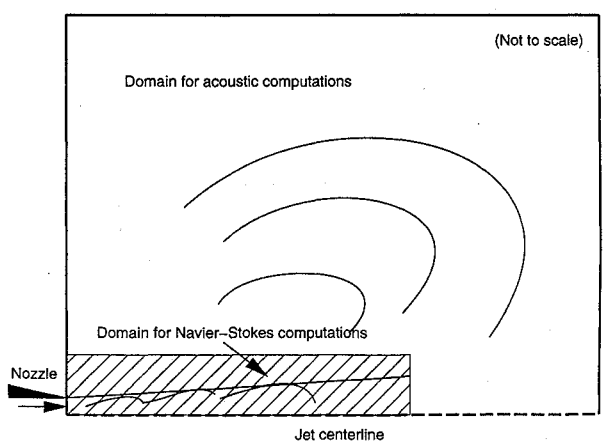

Fig. 2 Schematic of the computational domains for mean flow and acoustic computations.

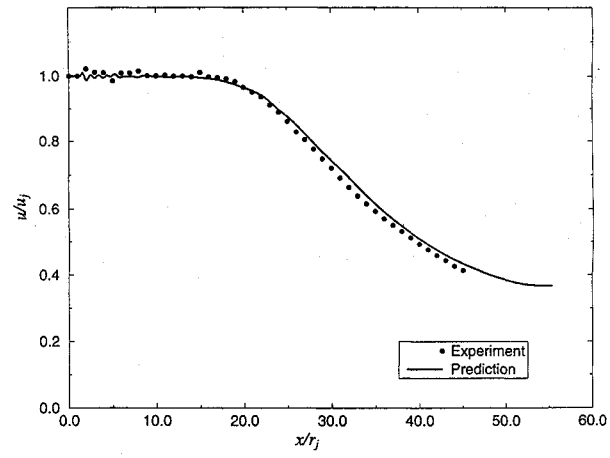

Fig. 3 Comparison of velocity distribution at the jet centerline; M_j = 2.0 and T_j = 755 K.

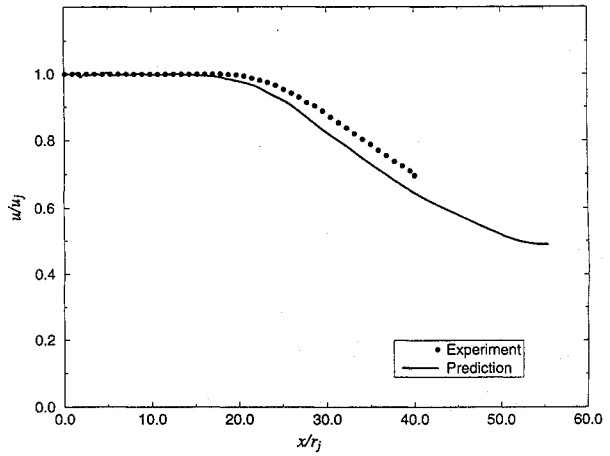

Fig. 4 Comparison of velocity distribution at the jet centerline; M_j = 2.0 and T_j = 313 K.

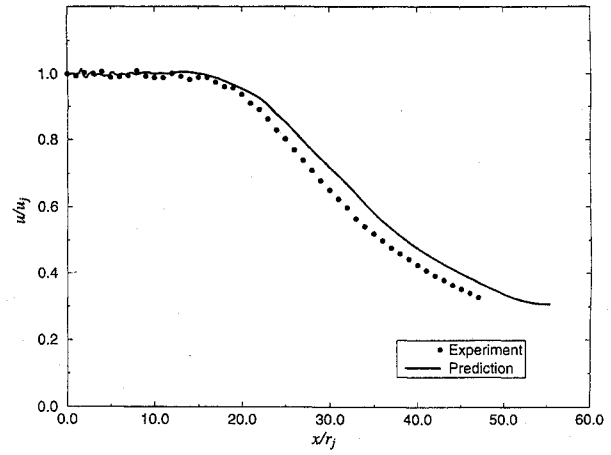

Fig. 5 Comparison of velocity distribution at the jet centerline; M_j = 2.0 and T_j = 1114 K.

The particular case of a Mach 2.0 jet at a jet total temperature of 755 K was chosen as the benchmark case. The three-zone turbulence model was calibrated to match the experimental data closely at this jet temperature. With the same set of constants, predictions of the mean flow were made at other jet total temperatures. Figures 3–5 show the predicted and measured centerline velocities for three different jet total temperatures of 755, 313, and 1114 K, respectively. In each case, the velocities have been normalized by the jet exit velocity. The empirical constants that appear in the model have been adjusted to match the measured values at 755 K, and this is reflected in Fig. 3. It can be seen that the predicted velocity decays at other temperatures are reasonably accurate, though the predicted potential core lengths are not that good. At the higher temperature of 1114 K, the predicted rate of mixing is lower than the measured mixing rate. But at the lower temperature of 313 K, this trend is reversed, and the predicted mixing rate is higher. There is, however, good qualitative agreement.

Some dynamic features of the flowfield are now presented. The Euler equations are also solved on an axisymmetric grid. As mentioned, both the linear and nonlinear forms may be solved. The eigenfunctions associated with the instability waves used to model the large-scale structures are prescribed at the upstream boundary. When the nonlinear terms are retained, the interactions between the various instability waves are taken into account. Five instability waves, consisting of the fundamental and the first four subharmonics, have been prescribed in the following test cases unless stated otherwise. Though the normalization condition provides a weighting factor for each instability mode, the initial amplitude distribution is not known. Tam[15] has pointed out the pitfalls associated with the use of discrete waves to model naturally occurring large-scale structures; the characteristics of naturally occurring turbulence structures are random, whereas the discrete instability waves are completely deterministic. To address this fundamental difficulty, Tam and Chen[27] developed a stochastic wave model in which the initial amplitudes are taken to be stochastic random functions. The characteristics of the large-scale structures in a two-dimensional mixing layer from such a representation were shown to provide good agreement with experimental measurements. In a recent study, Bechara et al.[8] used a stochastic description of the turbulence field by synthesizing the velocity field at each spatial location and for all time with a collection of discrete Fourier modes. The synthesized field described the noise source terms, and a system of linearized Euler equations were solved for noise predictions. This formulation was shown to provide realistic pressure signals and power spectral densities in the near field.

This level of sophistication and complexity is not attempted in the present study. Instead, a few discrete modes are used to model the large structures. This description is more appropriate for excited jets, where the excited large-scale structures when modeled with a single instability wave provided very good comparison with experiment, see Tam and Morris[28] and Gaster and Wygnanski.[29] In the simple approach here, the initial amplitudes of all of the instability waves are assumed to be equal. An initial value of 0.01 has been specified at the upstream boundary for the results reported here.

The Euler equations for the perturbations are solved, and the instantaneous values of the flow variables are obtained with the addition of the calculated mean values. Mankbadi et al.[7] demonstrated the wavelike nature of the flow structure to both random and harmonic initial conditions. In this study, since the eigenfunctions are used as initial conditions, the large-scale structures should be better characterized. Typical results from the nonlinear axisymmetric simulations are shown. The test case chosen is the Mach 2.0 jet at a total temperature of 755 K. The instantaneous spanwise vorticity contours at different times are shown in Fig. 6. These times correspond to $t = 0, T/8, 2T/8$, and $3T/8$, where T is the time period of the lowest subharmonic prescribed. The initial mixing layer seems to roll up into the cat's eye structure, after the instability waves have interacted and attained a sufficient amplitude. The vortex merging process is not readily observed in a round jet, unlike the case of a plane mixing layer. First of all, helical modes are dominant at higher Mach numbers, and second, the vortex merging process is not as organized as in a plane mixing layer.

A better visual picture of the turbulence structure is obtained when the radial velocity contours are examined. Such a time sequence is depicted in Fig. 7, with the nondimensional times being the same as those in Fig. 6. The same contour levels have been plotted for different times. There are several well-defined closed contours at all time frames. Close to the nozzle exit, there is a rich variety of structures, but farther downstream there are larger structures with increased spacing between them. When the pressure or density field is examined, there is a well-defined near field, and the orientation of the wavefronts is in good agreement with the schlieren pictures of the wave patterns associated with the Kelvin–Helmholtz instability waves; see Oertel.[30]

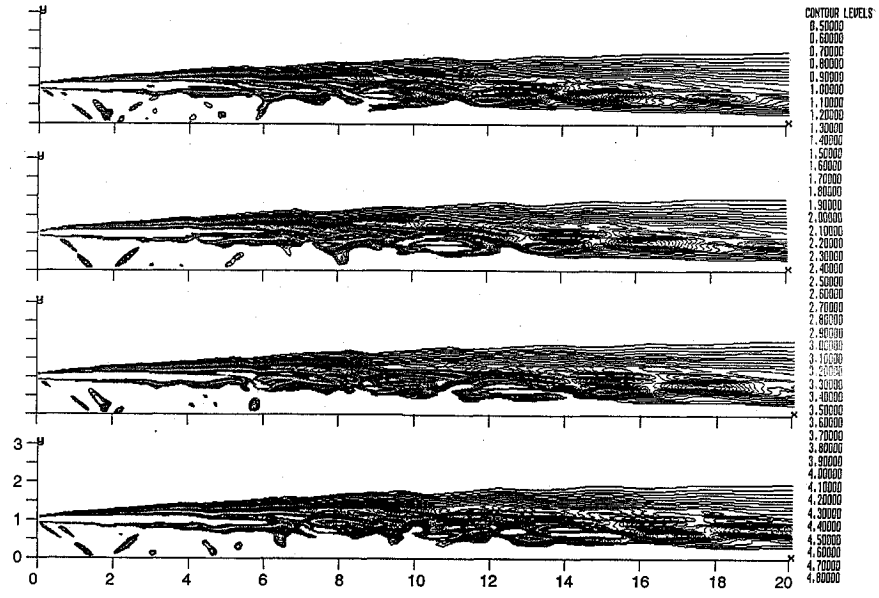

Fig. 6 Spanwise vorticity contours at four time levels.

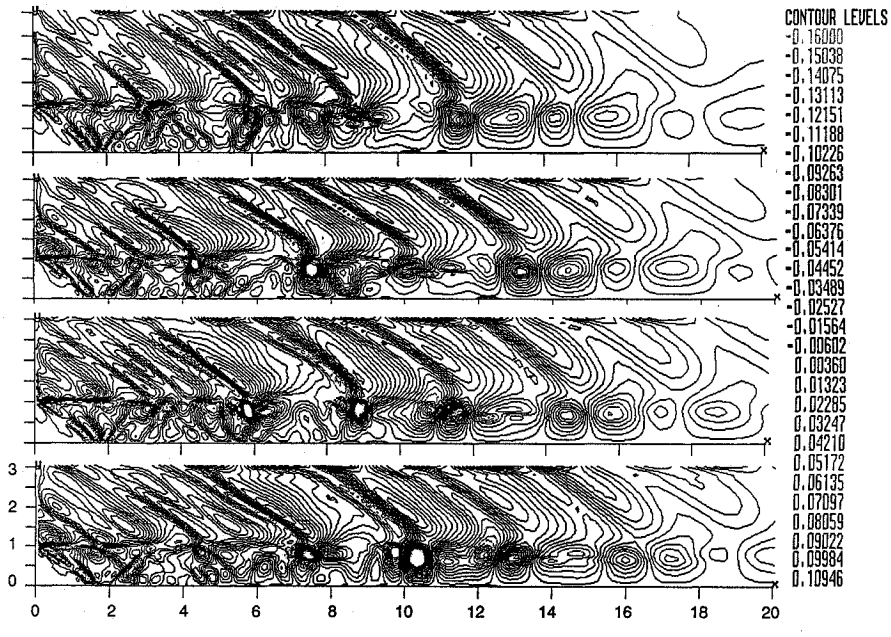

Fig. 7 Time sequence of radial velocity contours.

A sample three-dimensional simulation has also been carried out to verify whether the jet would lock on to the excited helical instabilities and to test the ability of the numerical scheme to resolve three-dimensional structures. For this case, 18 azimuthal planes, each 20 deg apart, were specified. Three axisymmetric ($m = 0$) instability modes and three helical ($m = +1$) modes were specified at the upstream plane. An instantaneous isosurface plot of the helicity density is shown in Fig. 8. Close to the nozzle exit, the axisymmetric modes seem to be dominant. Farther downstream, there is a well-defined helical structure. For the Mach number considered, experimental results have shown that the helical modes are more important than the axisymmetric modes. The current simulation is in qualitative agreement with experiments and captures the helical nature of the large-scale structure.

Prediction of Radiated Noise

For the noise predictions, a uniform grid is used both in the axial direction and in the radial direction beyond the first four jet radii. In the radial direction, a smaller grid size is specified for the first four jet radii so as to provide a good description of the mean flowfield and also to capture the peaks in the eigenfunction distributions. The computational domain extends to 100 jet radii both in the axial and radial directions, and the computations are carried out in the transformed coordinate system. Again, only three azimuthal planes are employed. This restricts the analysis to axisymmetric instability modes in the prescription of the large-scale structures, as a fully three-dimensional simulation is necessary to resolve higher azimuthal modes. Experimental studies as well as hydrodynamic stability analyses have shown that the $m = +1$ helical mode is dominant above a jet Mach number of about 1.4. In this preliminary simulation, only axisymmetric modes are considered. Issues such as numerics, prescription of appropriate boundary conditions, choice of a suitable numerical scheme, etc., will be addressed and resolved for the axisymmetric case before three-dimensional noise simulations are taken up. Because of this restriction, direct comparison with experimental measurements is not possible at the current stage. The computations are carried out for several time periods of the lowest subharmonic and a root-mean-square value of the fluctuation pressure is obtained during the last cycle. The computer time required for a simulation depends on the grid used as well as on the

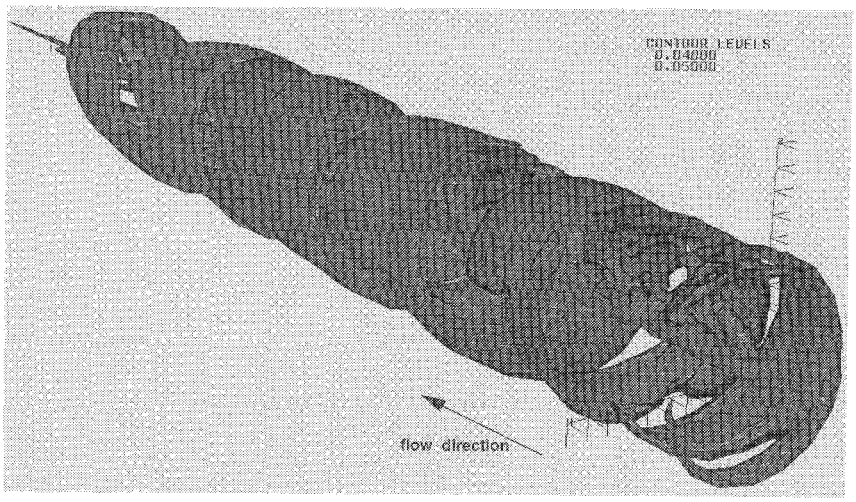

Fig. 8 Isosurface plot of helicity density; $M_j = 2.0$ and $T_j = 755$ K.

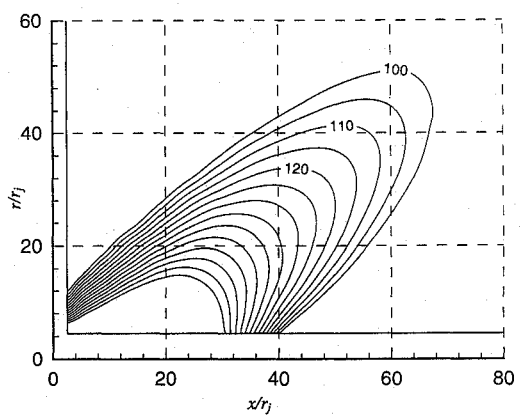

Fig. 9 Contour plot of sound pressure levels in decibels; $M_j = 2.0$ and $T_j = 755$ K.

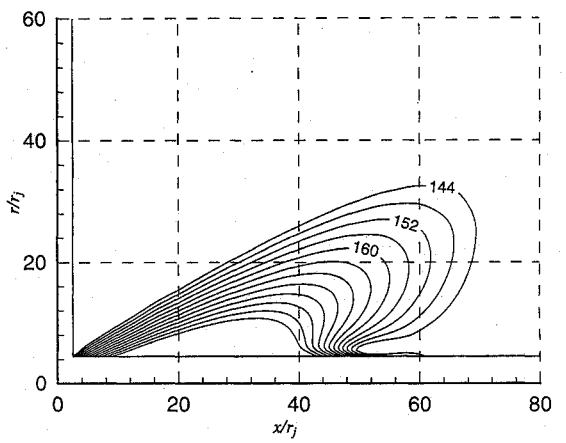

Fig. 10 Contour plot of sound pressure levels in decibels; $M_j = 2.0$ and $T_j = 313$ K.

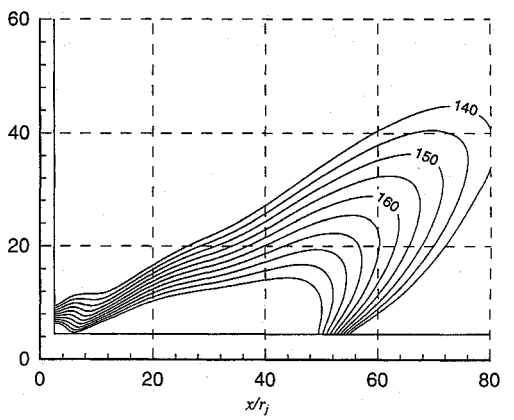

Fig. 11 Contour plot of sound pressure levels in decibels; $M_j = 2.0$ and $T_j = 1370$ K.

jet operating conditions for the acoustic computations. Typical CPU times are as follows: the mean flow computations require about 3 h of Cray Y-MP time and the acoustic computations about 14 h. Three-dimensional simulations require significantly larger run times.

Figure 9 shows contours of equal sound pressure levels for the Mach 2.0 jet at 755 K total temperature. The absolute levels cannot be predicted because of the prescription of an arbitrary initial amplitude for the instability waves. Therefore, the levels should be interpreted in a relative sense. The sound pressure levels have been scaled, with a scaling factor obtained by setting the pressure level to 148 dB at a distance of 30 and 20 radii from the nozzle exit in the axial and radial directions, respectively. There is a well-defined directivity pattern, and the peak angle is around 45 deg from the jet exhaust axis. The measurements of Seiner et al.[26] showed a peak between 45 and 46 deg, and there is good agreement between the predicted and the measured peak directivity angle. Perhaps this is not unexpected because the mean flowfield has been calibrated to very closely match the experimental data and then used in the calculation of the radiated noise. Apart from this, the prescription of the eigenfunctions of the instability waves at the upstream boundary seems to describe the evolution of the large-scale structures well and capture their radiated noise.

Figure 10 shows similar results for the Mach 2.0 jet at 313 K total temperature. There is a well-defined directivity pattern with a peak angle of about 35 deg. The data of Seiner et al.[26] showed a peak at 35 deg. Again, the predicted peak emission angle is in good agreement. Seiner and Ponton[31] have made detailed near-field acoustic measurements of unheated jets and have provided contour plots of the sound pressure levels. The predicted radiation pattern is very similar to the measurements from a Mach 2.0 unheated jet; see Fig. 25a in Ref. 31. As the jet temperature increases, the convective Mach number increases and the peak emission angle measured from the jet exhaust angle increases. This trend, which has been observed in the experiments, is reproduced in the current computations.

The case of a jet operating at a highly elevated temperature of 1370 K is considered next. Figure 11 shows the contours of equal pressure levels, with a predicted directivity angle of about 46 deg. The measurements of Seiner et al.[26] exhibited a major peak at 51 deg and a second peak at 43 deg. These two peaks were thought to be associated with the Kelvin–Helmholtz and the supersonic instability waves, respectively. In the present simulations only axisymmetric Kelvin–Helmholtz instability waves were introduced at the upstream boundary. This is not adequate at high jet temperatures, where the higher order instability modes are important contributors to the overall noise.

Seiner et al.[32] used the compressible Rayleigh equation to predict the Mach wave emission process from high-temperature supersonic jets. They were able to infer many of the important features of the radiated sound field with this approach. It was shown that at very low Strouhal numbers, the $m = \pm 1$ mode gave the correct angle of emission. Axisymmetric structures were important only at high Strouhal numbers. Therefore, the present simulation, though in good qualitative agreement vis a vis emission angle predictions, is only the first step in the direct computation of radiated noise.

The choice of Strouhal numbers for the description of the large-scale structures needs to be more comprehensive. Though the prescription of the fundamental and its subharmonics may be adequate in the simulation of jet mixing, these frequencies may not be the dominant ones in noise radiation, as pointed out by Tam.[33] The evaluation of the total growth integral (see Seiner et al.[32]) would provide the range of Strouhal numbers that are important for noise emission. A broadband model that encompasses a broad range of frequencies and azimuthal mode numbers would be appropriate, especially at high jet temperatures. Recently, Tam and Chen,[4] in their development of a broadband jet noise theory, evaluated the contributions of higher order modes to the turbulent mixing noise and showed that no single wave mode is the dominant source of noise for the Mach 2.0 jet at a total temperature of 1114 K. The contributions from different modes were shown to be responsible for the noise directivity curve to be fairly broad. This could explain the discrepancy for the highly heated jet case and points to the need for a broadband model. The assumption of equal initial amplitudes for all of the instability modes is not adequate. The recent stochastic model of Tam and Chen[4] for turbulent mixing noise allows the relative amplitudes of different instability modes to be determined. This complex problem cannot be easily addressed, especially for naturally evolving jets. A stochastic approach is clearly warranted for this case. In spite of the simplifying approximations, the present study has provided a qualitative measure of the Mach wave emission process of a supersonic jet.

Summary

A numerical technique for the computation of flow generated noise has been presented. Both the mean flow and the noise radiation phenomena have been simulated. The mean flow established with the solution of the Navier–Stokes equations has been used in conjunction with a linear/nonlinear Euler solver for the prediction of near-field noise. For the jet noise problem, the eigenmodes associated with the most amplified frequency at the nozzle exit and its subharmonics have been prescribed as the inflow conditions. However, only axisymmetric instability waves have been included in the noise calculations. This was dictated by considerations of large computation times required for three-dimensional simulations. In spite of the many simplifying assumptions, the present study has provided a qualitative study of the Mach wave emission process in a supersonic jet. The experimentally observed variation in the peak emission angle with jet temperature is correctly reproduced in the current computations. Most of the past jet noise predictions were based on the instability wave theory. In the present computations, the radiated noise is directly computed from the governing equations for the flow fluctuations. This approach represents one of the few recent attempts to apply computational aeroacoustics techniques for practical problems.

The hybrid method outlined in this paper is not geometry dependent and may be applied to several computational aeroacoustics problems, for example, Lim et al.[34] However, the mean flow must be obtained from a turbulence closure scheme that does not require the adjustment of empirical constants for different flow situations and geometries. Large eddy simulations offer the best prospect for the near future, and LES may be coupled to a higher order numerical scheme for the resolution of the perturbation quantities. Nonreflective boundary conditions are necessary so that any spurious reflections or errors that may be introduced at the boundaries do not propagate to the interior and contaminate the solutions. These outstanding issues need to be addressed before a truly direct noise prediction scheme can be developed.

Acknowledgments

This work was supported by the Lockheed Aeronautical Systems Company under an Independent Research and Development program. The authors would like to thank the NAS program for providing computer time on their supercomputer system. The first author gratefully acknowledges the valuable discussions with P. J. Morris throughout this study.

References

[1]Tam, C. K. W., and Morris, P. J., "The Radiation of Sound by Instability Waves of a Compressible Plane Turbulent Shear Layer," *Journal of Fluid Mechanics*, Vol. 98, Pt. 2, 1980, pp. 349–381.

[2]Tam, C. K. W., and Burton, D. E., "Sound Generated by Instability Waves of Supersonic Flows, Pt. 2, Axisymmetric Jets," *Journal of Fluid Mechanics*, Vol. 138, Jan. 1984, pp. 273–295.

[3]Tam, C. K. W., "Stochastic Model Theory of Broad Band Shock Associated Noise from Supersonic Jets," *Journal of Sound and Vibration*, Vol. 116, No. 2, 1987, pp. 265–302.

[4]Tam, C. K. W., and Chen, P., "Turbulent Mixing Noise from Supersonic Jets," *AIAA Journal*, Vol. 32, No. 9, 1994, pp. 1774–1780.

[5]Scott, J. N., "Acoustic Analysis using Numerical Solution of Navier–Stokes Equations," AIAA Paper 92-0506, Jan. 1992.

[6]Hardin, J. C., and Pope, D. S., "Sound Generation by Flow Over a Two-Dimensional Cavity," *AIAA Journal*, Vol. 33, No. 3, 1995, pp. 407–412.

[7]Mankbadi, R. R., Hayder, M. E., and Povinelli, L. A., "Structure of Supersonic Jet Flow and its Radiated Sound," *AIAA Journal*, Vol. 32, No. 5, 1994, pp. 897–906.

[8]Bechara, W., Bailly, C., Lafon, P., and Candel, S. M., "Stochastic Approach to Noise Modeling for Free Turbulent Flows," *AIAA Journal*, Vol. 32, No. 3, 1994, pp. 455–463.

[9]Dahl, M., and Morris, P. J., "Noise Radiation by Instability Waves in Coaxial Jets," AIAA Paper 94-2190, June 1994.

[10]Dash, S. M., Sinha, N., York, B. J., Kenzakowski, D., and Lee, R., "Computer Codes for HSCT Exhaust Flowfield Simulation and Observations on Turbulence Modeling," AIAA Paper 91-3297, Sept. 1991

[11]Mitchell, B. E., Lele, S. K., and Moin, P., "Direct Computation of the Sound Generated by Vortex Pairing in an Axisymmetric Jet," AIAA Paper 95-0504, Jan. 1995.

[12]Lyrintzis, A. S., and Mankbadi, R. R., "On the Prediction of the Far-Field Jet Noise Using Kirchhoff's Formulation," AIAA Paper 95-0508, Jan. 1995.

[13]Sankar, L. N., Reddy, N. N., and Hariharan, N., "A Comparative Study of Numerical Schemes for Aero-Acoustic Applications," *Proceedings of the ASME Forum on Computational Aeroacoustics and Hydroacoustics*, FED-Vol. 347, 1993, pp. 35–40.

[14]Gottlieb, D., and Turkel, E., "Dissipative Two-Four Methods for Time-Dependent Problems," *Mathematics of Computation*, Vol. 30, No. 136, 1976, pp. 703–723.

[15]Tam, C. K. W., "Jet Noise Generated by Large Scale Coherent Motion," *Aeroacoustics of Flight Vehicle: Theory and Practice*, NASA RP-1258, Aug. 1991, Chap. 6.

[16]McLaughlin, D. K., Morrison, G. L., and Troutt, T. R., "Experiments on the Instability Waves in a Supersonic Jet and Their Acoustic Radiation," *Journal of Fluid Mechanics*, Vol. 69, Pt. 1, 1975, pp. 73–95.

[17]Morrison, G. L., and McLaughlin, D. K., "The Noise Generation by Instabilities in Low Reynolds Number Supersonic Jets," *Journal of Sound and Vibration*, Vol. 65, No. 2, 1979, pp. 177–191.

[18]Troutt, T. R., and McLaughlin, D. K., "Experiments on the Flow and Acoustic Properties of a Moderate-Reynolds-Number Supersonic Jet," *Journal of Fluid Mechanics*, Vol. 116, March 1982, pp. 123–156.

[19]Seiner, J. M., McLaughlin, D. K., and Liu, C. H., "Supersonic Jet Noise Generated by Large-Scale Instabilities," NASA TP-2072, Sept. 1982.

[20]Tam, C. K. W., Chen, P., and Seiner, J. M., "Relationship Between Instability Waves and Noise of High Speed Jets," *AIAA Journal*, Vol. 30, No. 7, 1992, pp. 1747–1752.

[21]Ho, C. M., and Huang, L. S., "Subharmonics and Vortex Merging in Mixing Layers," *Journal of Fluid Mechanics*, Vol. 119, June 1982, pp. 443–473.

[22]Morris, P. J., Giridharan, M. G., and Lilley, G. M., "On the Turbulent Mixing of Free Shear Flows," *Proceedings of the Royal Society of London, Series A: Mathematical and Physical Sciences*, Vol. 431, 1990, pp. 219–243.

[23]Viswanathan, K., and Morris, P. J., "Predictions of Turbulent Mixing in Axisymmetric Compressible Shear Layers," *AIAA Journal*, Vol. 30, No. 6, 1992, pp. 219–243.

[24]Dash, S. M., Sinha, N., and Kenzakowski, D. C., "The Critical Role of Turbulence Modeling in the Prediction of Supersonic Jet Structure for Acoustic Applications," *Proceedings of the DGLR/AIAA 14th Aeroacoustics Conference*, DGLR-Bericht 92-03, 1992, pp. 643–654.

[25]Pope, S. B., "An Explanation of the Turbulent Round-Jet/Plane-Jet Anomaly," *AIAA Journal*, No. 3, 1978, pp. 279–281.

[26]Seiner, J. M., Ponton, M. K., Jansen, B. J., and Lagen, N. T., "The Effects of Temperature on Supersonic Jet Noise Emission," *Proceedings of the DGLR/AIAA 14th Aeroacoustics Conference*, DGLR-Bericht 92-03, 1992, pp. 295–307.

[27]Tam, C. K. W., and Chen, K. C., "A Statistical Model of Turbulence in Two-Dimensional Mixing Layers," *Journal of Fluid Mechanics*, Vol. 92, Pt. 2, 1979, pp. 303–326.

[28]Tam, C. K. W., and Morris, P. J., "Tone Excited Jets, Pt V: A Theoretical Model and Comparison with Experiment," *Journal of Sound and Vibration*, Vol. 102, No. 1, 1985, pp. 119–151.

[29]Gaster, M., Kit, E., and Wygnanski, I., "Large-Scale Structures in a Forced Turbulent Mixing Layer," *Journal of Fluid Mechanics*, Vol. 150, Jan. 1985, pp. 23–39.

[30]Oertel, H., "Mach Wave Radiation of Hot Supersonic Jets," *Mechanics of Sound Generation in Flows*, edited by E. A. Muller, Springer, Berlin, 1979, pp. 275–281.

[31]Seiner, J. M., and Ponton, M. K., "Aeroacoustic Data for High Reynolds Number Supersonic Axisymmetric Jets," NASA TM-86296, Aug. 1985.

[32]Seiner, J. M., Bhat, T. R. S., and Ponton, M. K., "Mach Wave Emission from a High Temperature Supersonic Jet," *AIAA Journal*, Vol. 32, No. 12, 1994, pp. 2345–2350.

[33]Tam, C. K. W., personal communications, Nov. 1993.

[34]Lim, T. B., Sankar, L. N., Hariharan, N., and Reddy, N. N., "A Technique for the Prediction of Propeller Induced Acoustic Loads on Aircraft Structures," AIAA Paper 93-4340, Oct. 1993.